

METHODS TO ASSESS BUBBLE SCREENS APPLIED TO MITIGATE SALT INTRUSION THROUGH LOCKS

by

Pepijn P.D. van der Ven^{1,2}, Tom S.D. O'Mahoney¹ and Otto M. Weiler¹

ABSTRACT

Salt intrudes into the freshwater system via shipping locks located at the sea every time these open the lock gate. With increasing lock size and increasing shipping traffic intensity, this issue requires attention. The application of bubble screens along the lock's entrance is one of the available mitigating measures. The effect of such a screen is often expressed as a factor reducing the speed of the lock exchange process: the so-called salt transmission factor, which may reach 0.25, depending on the bubble screen design and operation. The effect on the salt intrusion during successive lockages may be enhanced further when the duration of the doors being open is minimized. This paper presents various methods to determine the effect of bubble screens on salt intrusion, a discussion on the assessment of its design with scale model tests or numerical computations as well as the effect of the salt intrusion on the inland water system.

1. INTRODUCTION

Salt intrusion and mitigating measures have been studied extensively in recent years. Shipping locks are a clear example of a location where salt intrusion via surface water would occur if not properly mitigated. The importance of mitigation is related to the required quality of the fresh water, for ecological reasons or due to its use for agriculture and/or drinking water.

Recent shipping traffic developments contribute negatively to salt intrusion unless proper mitigating measures are taken. Increasing shipping intensity demands more frequent lockages, with every lockage adding to the amount of salt intrusion through the lock. Furthermore, the enormous size of modern locks means they contain a large amount of salt water that potentially flows towards the inland water bodies. Sea level rise as a result of climate change also leads to higher water levels at sea locks and increasing salt intrusion. Similarly an increasing strain on freshwater resources requires that more attention is given to issues concerning water quality. This can also lead to less water being available for some mitigation measures, such as flushing of water through locks and sluices.

The research on salt intrusion through shipping locks has led to computational methods to model the exchange of water in the vicinity of the lock and the (ongoing) development of the coupling with regional models.

Furthermore, the studies have increased the knowledge of various salt intrusion mitigating measures – in particular the bubble screen, being the specific topic of this paper. Bubble screens are applied at shipping locks between salt and fresh water bodies, in order to decrease the rate of salt intrusion as a result of the locking process. Various measurements have been performed in the past decades to address the effectiveness of bubble screens in shipping locks. The potential of bubble screens is currently given a renewed assessment due to the developments mentioned above.

¹ Deltares, The Netherlands

² Corresponding author, pepijn.vanderven@deltares.nl

Other mitigating measures include the application of freshwater flushing discharge through the lock (Weiler et al., 2015) or selective withdrawal using a hydraulic structure (Boschetti et al., 2017). Changes in operation (e.g. keeping the lock gates closed as much as possible) may also reduce salt intrusion, as will be explained in this paper.

Compared to the application of a freshwater flushing, bubble screens are more expensive as the required air flow rate and pressure demand a significant compressor size. An important question therefore is to optimize the design or use of the bubble screen such that the required salt intrusion reduction is met at a minimum use of energy. The question how the bubble screen technology scales up towards the larger depths of modern locks should also be explored. Recent work, presented in this paper, has focused on the application of various research methods to contribute to these questions.

2. GENERAL CONSIDERATIONS OF THE LOCK EXCHANGE

2.1 Driving parameters of lock exchange

The salt intrusion through a lock during a day of lockages is determined by the number of lockages and the salt intrusion for each of these lockages. More shipping traffic leads, in general, to more lockages which leads to more salt intrusion. The number of lockages depends on the traffic passing the lock, which has a highly stochastic nature, and on how the lockkeeper handles this traffic. The lock operator decides, for example, how many ships are dealt with in one lockage.

The amount of salt intrusion per lockage depends on the salinity difference between the lock chamber and the approach harbour, as well as the water level and depth, the lock size and the duration of the gates being open.

Two types of processes contribute to salt intrusion through locks. The first one is the salt carried inland by the lockage prism, applicable in cases where the water level at the salt water side is higher than that at the freshwater side. The volume of the lockage prism is equal to the product of length and width of the lock chamber and the difference in water level. In delta areas, where salt and fresh water meet, the latter is usually relatively small.

The second contribution is related to the process of lock exchange: the exchange flow between the lock chamber and the approach harbour (at either side, one after the other) due to the difference in density of the salt and fresh water. Given sufficient time, this process will result in (almost) the entire volume of the lock chamber exchanging between both sides of the lock. Equal volumes of water will be exchanged in both directions, but due to the difference in salinity, a quantity of salt will move inland which is related to the volume of the lock, not the lockage prism. As the lock volume is usually much larger than the locking prism, lock exchange is often the dominant factor contributing to salt intrusion.

The evolution of a density current in a lock exchange in time (see Figure 1), for saltwater called the salt wedge, is well studied (Shin et al., 2004). The salt wedge initially extends over approximately half the depth H and has an initial velocity c_i which is related to the depth and the density difference as given in (1).

$$c_i = \frac{1}{2} \sqrt{g \frac{\Delta \rho}{\rho} H} \quad (1)$$

In which

g gravitational constant, 9.81 [m/s²]
 $\rho, \Delta \rho$ density, density difference between lock chamber and approach harbour [kg/m³]
 H water depth [m]

It is clear from this formula that the amount of salt water which enters the inland waterway when the lock gate is opened increases when the density differences increases and when the water depth increases. Here an open, unhindered lock exchange is considered with unlimited water bodies on both sides.

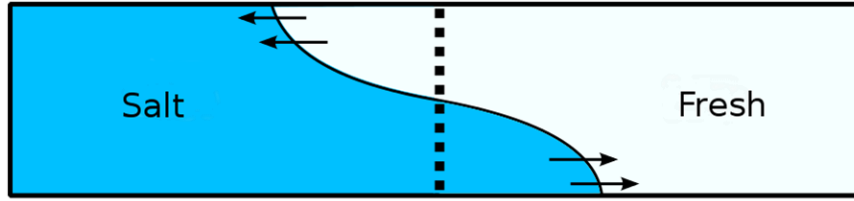


Figure 1: Schematic illustration of a lock exchange

When aiming to describe the process of lock exchange in practice, accounting for the finite volume of the lock and the operation of the lock gates, the formulation as proposed by Van den Burgh and De Vos (1962) and Vrijburcht et al. (2000) is most convenient. In this formula the relative lock exchange is given by (2).

$$U = \tanh\left(\frac{T_{\text{open}}}{T_{\text{LE}}}\right) \quad (2)$$

In which

- U relative lock exchange, i.e. the exchanged volume as a ratio of the volume of the lock [-]
- T_{open} the duration of the doors being open [s]
- T_{LE} the 'theoretical' duration for a total lock exchange [s]

The theoretical duration for a total lock exchange, T_{LE} , is the time needed for the salt wedge (or the fresh wedge, depending on the lock head) to travel into the lock and back to the open door after reflecting at the closed end, assuming the initial velocity c_i as constant. This period is given by the following formula.

$$T_{\text{LE}} = \frac{2L}{c_i} = \frac{2L}{\frac{1}{2}\sqrt{g\frac{\Delta\rho}{\rho}H}} \quad (3)$$

In which

- L length of lock chamber [m]
- c_i the initial velocity [m/s]

In many locks between salt and fresh water the value of T_{LE} is in the range of typical gate open times, leading to values of $T_{\text{open}}/T_{\text{LE}}$ in the range of 0.5 to 2.0.

2.2 Effect of bubble screens in the relative lock exchange

The effect of a bubble screen is that it hinders the process of lock exchange, reducing the mass flow rate of salt associated with it. The effect is quantified in the salt transmission ratio, η . The value of η that is achieved by a bubble screen is determined by the air flow rate, the depth of water in the lock head and the density difference between lock chamber and approach harbour. The factor has been determined for various mitigating measures in in-situ measurements (see Paragraph 4.1). Sometimes reference is made to a reduction factor but this is simply $1-\eta$.

The theory behind this goes back to Abraham and Van den Burgh (1962). This salt transmission ratio reduces the exchange of water through the lock head and increases the time required for the (complete) exchange of the water in the lock, T_{LE} , with a factor $1/\eta$.

Introducing this salt transmission ratio into (2) changes to the following equation.

$$U = \tanh\left(\frac{\eta T_{open}}{T_{LE}}\right) \quad (4)$$

In which

η the salt transmission factor [-]

In this expression the meaning and value of T_{LE} remain unchanged; it does not include the effect of the bubble screen, but is based only on dimensions of the lock and the densities of water inside and outside of the lock.

The process in time related to this formulation is given in Figure 2, for two situations: one without a bubble screen, and one with a bubble screen with $\eta = 0.4$.

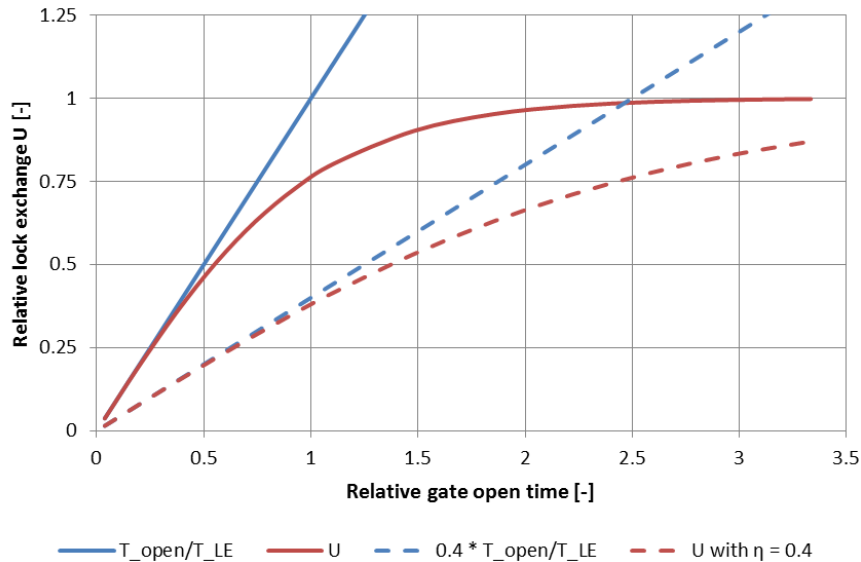


Figure 2: Relative lock exchange (U , red lines) as a function of the relative gate open time, showing an unprotected lock head (continuous lines) and a lock head with bubble screen (dotted lines)

Note that, in the case without bubble screen, when T_{open}/T_{LE} is 1, the lock exchange as described by (4) is about 76% complete. When applying a bubble screen with an η of 0.40 the lock has been exchanged at this time only 38%.

It is essential to understand, as is also shown in Figure 2, that the bubble screen reduces the speed of the lock exchange, but does not stop the process. This means that a bubble screen can only be effective when it goes hand-in-hand with restricting the time that the lock gates are open.

2.3 Application of bubble screens at both lock heads: effect on salt intrusion

The effect of a bubble screen becomes much stronger when it is applied at both lock heads. After a partial lock exchange with one of the approach harbours, the lock turns towards the other approach harbour, but due to the partial lock exchange over one lock head the density difference over the other lock head is smaller, reducing the speed of the lock exchange. Disregarding the effect of a difference in water level over the lock, the salinity and density in the lock chamber will vary around the mean of the values in both approach harbours after a number of cycles.

This variation of the salinity inside the lock chamber (i.e. maximum – minimum value of salinity) will be smaller than the difference in salinity at both sides of the lock and this ratio is a direct measure for the amount of salt transported through the lock per complete lock cycle (including both an upward and a downward lockage). This defines the parameter Z , the relative salt transport, being the ratio between the variation of salinity inside the lock and the difference in salinity at both sides outside the lock, see (5). It is an equilibrium value, reached after a (large) number of lock cycles with equal gate open times at both lock heads, in absence of a level difference over the lock.

$$Z = \frac{\Delta S_{\text{variation inside the lock}}}{\Delta S_{\text{conditions outside the lock}}} \quad (5)$$

In which

ΔS difference in salinity (see text) [kg/m³]

Knowing Z makes it easy to calculate the transport of salt through a lock, using (6).

$$\dot{M} = N \cdot Z \cdot \Delta S_{\text{conditions outside the lock}} \cdot V_{\text{lock}} \quad (6)$$

In which

\dot{M} the mass flux of salt per unit of time [kg/s]

N the number of complete lock cycles (up and down) per unit of time [1/s]

V_{lock} the volume of the lock chamber [m³]

The value of Z has been calculated for a range of values and is shown below. Just like U (the relative lock exchange) the value of Z (the relative salt transport), is highly sensitive to the gate open times, which, together with a bubble screen, are essential to limit the lock exchange each time the gates are open at one of the lock heads.

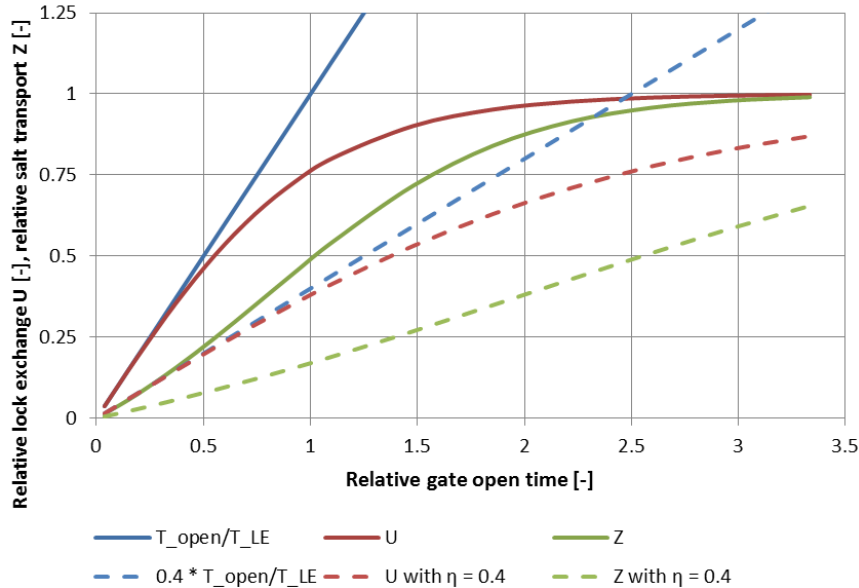


Figure 3: Relative lock exchange (U , red lines) and relative salt transport (Z , green lines) as a function of the relative gate open time, showing an unprotected lock head (continuous lines) and a lock head with bubble screen (dotted lines)

As shown in Figure 3, the application of bubble screens with a certain value of η in both lock heads reduces the salt intrusion when compared to the application in one lock head only (assuming complete lock exchange in the other, unprotected lock head). Note that this reduction is achieved by

a smaller variation of salinity in the lock chamber, which leads to smaller difference in density over each lock head, which in turn reduces the air flow needed to achieve the value of η . So a larger reduction of salt intrusion can be reached, with a smaller capacity of air compressors. This explains why, although these compressors have to run during a larger period of time (when either of the lock heads is open), it is generally favourable to apply bubble screens at both lock heads.

3. DETAILED SIMULATIONS OF LOCKING CYCLE AND SALT DISPERSION

3.1 Simulating the locking process

As the graphs and formulae in Section 2 show, the lock operation is a very important factor in the amount of salt intrusion and it implies that the lockkeeper is not only facilitating navigation, but is also controlling salt intrusion. Achieving a restriction in the time that the lock gates are open for ships can be difficult because the lock keeper has to balance these completely different interests. In some cases a large gate open time may be demanded for the safety of the operation, for instance when a large vessel approaches a sea lock, it may want to see the gate open in order to be sure that the manoeuvre does not have to be interrupted.

Furthermore, the lock utilization is highly variable, with variations in occupancy during the day or the night, with the tide at the sea-side, with variations over days of the week and over the seasons of the year. The vessel traffic may be asymmetrical, with one direction being dominant during part of the day or week, and the other direction at other times.

For the calculation of the salt intrusion in such varying conditions, and for varying applications of mitigating measures, the lockage process has been implemented in the computational program WANDA-Locks, which is embedded in WANDA, a one-dimensional program originally developed for complex systems of pipeline flow (see reference website), allowing a generic and explicit modelling method. The program has been validated using measurements at the Stevin Locks (De Groot, 2015) and the Krammer Locks (Weiler et al., 2015).

WANDA-Locks uses formulae for salt intrusion based on Uittenbogaard (2010) , including the impact of mitigating measures such as bubble and water screens by the salt transmission factor η that was introduced in Paragraph 2.2. The salt transport resulting from the levelling flow is taken into account by setting the hydraulic components (e.g. valves) according to locking procedures and having these being triggered by the actual water level in the lock. This ensures a realistic modelling of the locking process, going through the lockage cycle step by step.

The procedure explicitly incorporates the considerations of the lockkeeper and allows the inclusion of the stochastic nature of traffic demand. The model can be fed by either registrations of lock operation, or by a simulated operation, generated by vessel traffic models such as SIVAK (De Gans, 2010). Details of this schematization are given in Van der Ven et al. (2015).

3.2 Far-field modelling

The most critical salinity value is generally situated somewhere upstream, at the location of an intake of fresh water for agriculture, industry or drinking water. This is where salinity has to be kept below a certain criterion value. Between the navigation lock, 'producing' the salt, and the freshwater intake various processes play a role, leading to a different (lower) salinity at the intake than close to the lock. These processes can include density flows in the freshwater system, vertical mixing due to shipping traffic and the discharge of water from upstream towards the lock.

These 'far field' processes need to be considered using suitable hydrodynamic models in order to establish the difference between the salinity at the intake and at the lock and how this varies with several conditions, especially with the discharge. Examples of such models are Delft-3D or SOBEK

(both developed by Deltares). These models should include the salt intrusion through locks and sluices (as well as outflow through these points) as boundary conditions. It must be emphasized that the coupling is two-way, as described in Paragraph 2.3: the actual salinity at both sides of the lock determines the salt intrusion through the lock. Therefore, a so-called online coupling or an iterative computation procedure should be applied.

A suitable set of formulae to include salt intrusion through locks in far-field models in an online manner is not yet available. In view of computational time it preferably does not require a very detailed simulation of the locking process occurring at these locks. The formulae outlined in the previous section should form the basis for this coupling and these are planned to be implemented in the Deltares software.

4. DETERMINATION OF THE SALT TRANSMISSION RATIO η

The salt transmission factor η , which is used in the formulae and models discussed in Section 3, can be studied in scale model tests, with numerical computations or in situ. These methods will be discussed in the present section.

4.1 In situ measurements

In situ measurements can be used to determine the salt transmission factor η that applies to the lock exchange rate when a bubble screen is used. The salt transmission factor is defined as the ratio of salt intrusion with measures versus the salt intrusion for the lock without measures. The salt intrusion is the increase of the total mass of salt in the lock chamber during the exchange period. This period is assumed to be the same for the situation with and without measures.

Determining this transmission factor in situ comprises of measurements of the total mass of salt in the lock chamber before opening the door and after closing the door. To do so, conductivity measurement instruments are installed in the lock chamber, typically at 20-25 locations, measuring salinities along verticals distributed over the lock chamber. This grid of data points is used to calculate the total mass of salt. Abraham and Van den Burg (1962) present such measurements performed at the locks of Kornwerderzand and IJmuiden (both in The Netherlands), with depths ranging between 5 and 10 m.

Further in situ measurements can be found in Uittenbogaard et al. (2015a) and Keetels et al. (2011), who present the application an innovative combination of bubble and water screens at the Stevin Lock (The Netherlands). The dimensions of this shipping lock are 148 m length, 14 m width and 4.7 m depth. The tests consider an improved design of the bubble screen, using regulators to create a uniform distribution over the lock width and a specific placement of the bubble caps to create a dense bubble screen.

Conductivity meters were positioned in the approach harbours and at five verticals in the lock chamber, with five measurement points per vertical. The water levels, valve positions, opening and closure of the lock gates, the type of ship in the lock chamber and other parameters were recorded as well. The measurements were performed while the lock was in operation, i.e. with traffic through the lock.

Figure 4 presents a selection of the results of the tests, taken from Uittenbogaard et al. (2015b). Results from Abraham and Van den Burg (1973) have been included in the same figure (black dots). The salt transmission factor decreases with increasing air flow rate and varies with the design and the combination of mitigating measures. Previous tests show a typical transmission factor of 0.40, where the new design and operation of the bubble screen are shown to be able to reach values as low as 0.25 ± 0.05 and even 0.15 ± 0.05 when a fresh water screen is used additionally (see Keetels, 2011).

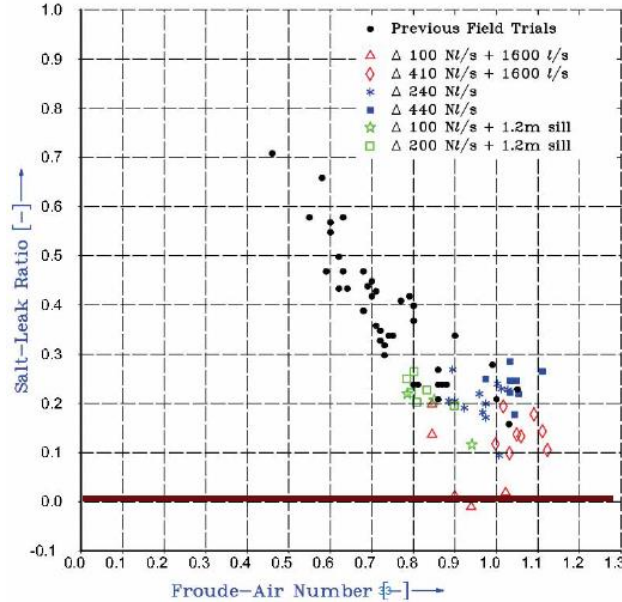


Figure 4: Results from in-situ measurements by Abraham and Van den Burgh (1973) and Uittenbogaard et al. (2015a) combined, showing the salt transmission factor η as a function of Froude air number (from Uittenbogaard, 2015b)

A similar design of bubble screen was tested subsequently at the Krammer recreational lock (The Netherlands) by Weiler et al. (2015), see Figure 5. The test set-up was similar to Uittenbogaard et al. (2015a), with an extensive grid of conductivity measurements in the lock and a detailed registration of lock operation. In contrast to the Stevin locks, the Krammer locks experience a tide of roughly 1.5 m amplitude (average condition). Furthermore, the Krammer makes use of a complex system of culverts to level the lock and to realize a flushing discharge, which were modelled using WANDA-Locks.

Tests included various bubble screen air flow rates and various combinations of mitigating measures: bubble screens, water screens and flushing discharge. The goal was not to find a single optimal setting of measures, but to assess the performance of several different settings. The availability of fresh water determines which setting to apply, e.g. using less flushing discharge in periods of a shortage of fresh water and compensating that with a higher bubble screen air flow rate. Lock operators were asked to perform measurements during night time, at strict 1 hour intervals, to facilitate the comparison of various settings of mitigating measures.

The measurements showed that the new system, using a bubble screen and flushing discharge, would sufficiently reduce salt intrusion. Furthermore, the measurement data was used to compare WANDA-Locks with and to identify required further developments of that model.

The pilot at the Krammer locks also evaluated the operational effects of a bubble screen: e.g. the ability for ships sailing into the lock to manoeuvre and to moor in the lock chamber. Furthermore, it focusses on the costs of conversion of the bigger commercial locks towards these innovative mitigation measures and the costs of operation of the bubble screens. These results have helped Rijkswaterstaat³ in their decision to apply bubble screens at the commercial locks of the Krammer lock complex; this project is to be executed in the coming two years.

³ Rijkswaterstaat is part of the Dutch Ministry of Infrastructure and the Environment and responsible for the design, construction, management and maintenance of the main infrastructure facilities in the Netherlands.



Figure 5: Bubble screen in the Krammer recreational lock (from Weiler et al., 2015)

The tests at the Krammer provided another determination of the bubble screen's salt transmission factor, i.e. the effect on the exchange rate during the lock exchange phase. Moreover, the tests provided a measurement of the effect of the application of bubble screens based on a standardized series of successive lockages.

4.2 Near-field scale model measurements

Paragraph 4.1 showed that a different design or operation of bubble screens can further reduce the transmission factors. This shows room for design and operation optimization: what would be the most efficient bubble screen? From the tests performed in the past it is assumed that an optimal bubble screen realizes (1) a uniform distribution of the air flow over the lock's width, (2) a uniform bubble size and thus uniform bubble rising velocity and (3) a dense bubble curtain without holes or openings. To determine design alternatives, it is obviously beneficial to be able to predict the performance of a bubble screen design before construction.

Scale model experiments provide a useful method for this assessment as, contrary to in-situ measurements, laboratory experiments allow good control of boundary conditions (e.g. water depth and salinity difference). Furthermore, scale model measurements can help to obtain a more detailed understanding of the physical processes of bubble screens as a salt intrusion mitigating measure, as laboratory tests generally allow more extensive measurements and visual inspections. These detailed observations are a required addition to theoretical studies, e.g. by Abraham et al. (1973), which provide excellent starting points.

Scale model research regarding bubble screens found in literature focus on several different topics, mostly on bubble screens in homogeneous water, e.g. to reduce wave penetration into port basins (e.g. Bulson, 1961). Scale model research on bubble screens to mitigate salt intrusion is rather scarce. This section presents a selection of such research.

Keetels et al (2011) have performed laboratory tests in preparation to the in-situ tests discussed in Paragraph 4.1. A flume approximately 0.30 m depth was used, consisting of a large compartment filled with salt water and a smaller compartment filled with fresh water. A gate in the flume separated the two compartments. The air injector, a perforated pipe of 1 cm diameter, was situated inside the saltwater reservoir near the gate. After the gate was opened, a gravity current started to enter the freshwater compartment while fresh water moved towards the saltwater compartment. Salinity was measured at two verticals, with 12 positions distributed per vertical. A lock-exchange experiment without any measures against salt intrusion was conducted for reference.

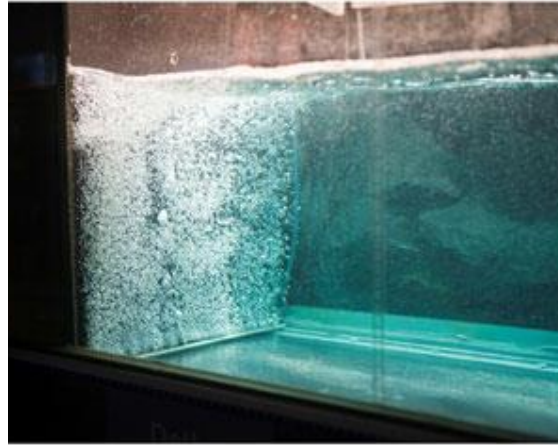


Figure 6: Closely packed air curtain in the laboratory (from Keetels et al., 2011)

Van der Ven and Wieleman (2017) present scale experiments of a bubble screen in a flume of 1 m depth and 1 m width. Their set-up is shown in Figure 7. The flow velocities were measured with electro-magnetic (EMS) instruments, which were installed to capture velocity components in the vertical as well as along the flume length. The instruments were moved in both the vertical and along the flume length to create a grid of measurement points. This measurement method could be used only since these experiments consider homogeneous water; the situation is assumed not to change in time. An important simplification is therefore that the performance of the bubble screen is evaluated only on the induced water motion.



Figure 7: Overview of scale model set-up by Van der Ven and Wieleman (2017): (a) bubble caps as built in the Kramer recreational lock; (b) caps used for the scale model of the bubble screen; (c) overview of the EMS instruments and bubble screen during a test condition

The results of Van der Ven and Wieleman (2017) show reasonable to good agreement with measurements done by Riess and Fanneløp (1998), who have considered a comparable small scale. Furthermore, the surface velocity shows good comparison to a full scale measurement performed by Bulson (1961). It is therefore concluded that the tests performed in this study are a reasonable representation of a real bubble screen. The accuracy of the measurements is a point of attention because of the limited accuracy of EMS instruments at the lowest flow velocities and the limited measurement duration per location. The measurements were performed in homogeneous water and

it is clear that, in order to assess the effect of a bubble screen as measure against salt intrusion, one should include the density difference in scale model tests.

Van der Ven and Oldenzien (2018) present recent scale model measurements that have been performed at Deltares. The goal of these experiments is to assess the difference in performance of varying bubble screen operation. As these differences may be subtle, measurements of high accuracy and at a high spatial resolution were required.

These tests too were at a small scale, having a flume of 2.40 m length, 0.50 m width and a water depth of 0.40 m. The set-up is shown in Figure 8. The flume was divided in two equal compartments by a metal sheet representing a lock door. One compartment was made saline and dyed blue, the other was kept fresh. As the door was lifted, a so-called lock exchange occurred, which was attenuated by the bubble screen. Air flow rate and bubble size were varied and tests were done with a density difference as well as in homogeneous fresh water.

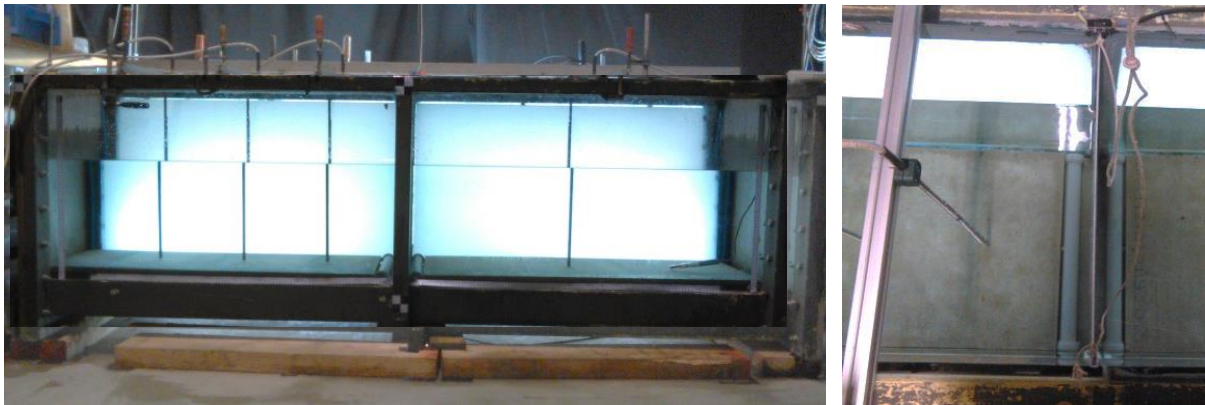


Figure 8: The setup used for the dye experiments; showing the tank of 2.40 m length, with four conductivity measurements rods clearly visible against the lit background (left) and the two bubble screen generators made from PVC-piles on either side of the separating sheet in the middle of the flume (right)

The experiments comprised two optical measurement techniques: (1) PIV measurements of the flow induced by the bubble screen (not shown here) and (2) the calibrated video-recording of the mixing induced by the screen and the exchange current by applying a dye to the salt water compartment.

The PIV measurements were performed in a separate tank with an identical geometry and for the homogeneous, fresh water cases only. The fields of view included the left hand side of the tank, including the bubble screen. An example of the velocity fields obtained in this way is given in Figure 9.

The dye recording was translated to a density map for every recorded time step. Three such maps are shown in Figure 10. The results provide insight in the several phenomena that occur: (a) the distribution of the entrained and mixed water over both compartments and (b) a density current on the flume floor due to a saline flow through the weaker lower part of the screen. Figure 11 shows the amount of dye within the left compartment, expressed as a percentage of the total mass of dye. This equals the salt fraction.

The two compartments can be interpreted as a lock chamber and an approach harbour. In Dutch reality, the approach harbour would not be confined, whereas the flume is obviously of limited dimension. This means that the sloshing seen in Figure 11 (black line) would not occur in reality and only the first approximately 20 seconds are representative. Note that the flume can however be seen to represent a sequence of locks chambers, e.g. the Panama locks.

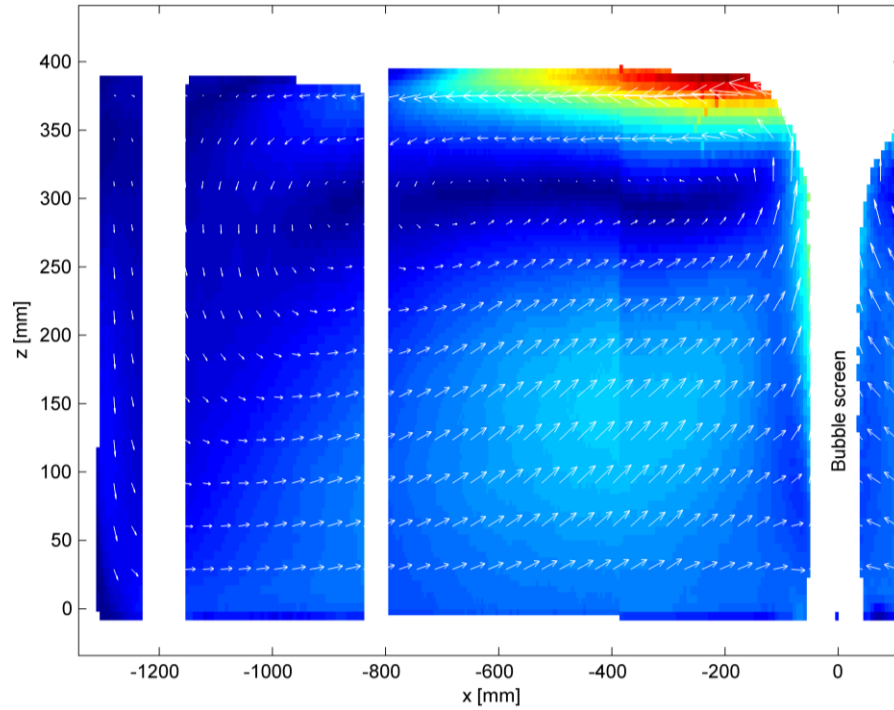


Figure 9: Induced flow velocities (colour shows magnitude) from a test in homogeneous water, on the left side of the bubble screen

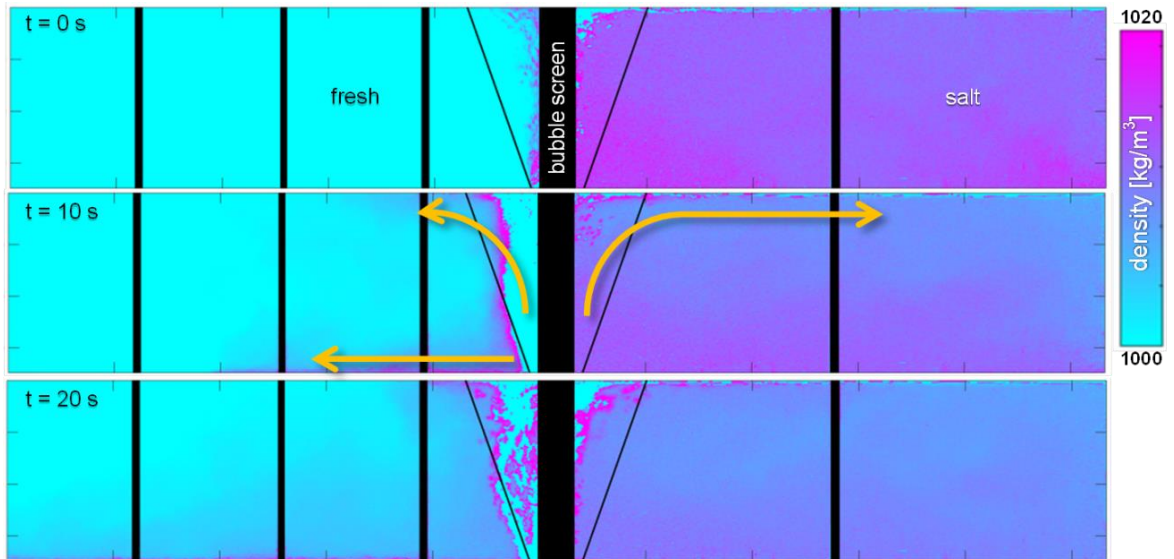


Figure 10: The exchange of fresh and saline water affected by the bubble screen, at various times after opening the lock door; from Van der Ven and Oldenziel (2018)

In Figure 11 the results of varying air flow rates (expressed in Froude air numbers, with $Fr_{air} \propto q_{air}^{1/3}$) are presented; multiple lines of the same colour denote repetitions of the same test. The situation without a bubble screen (black line) shows the sloshing of the unhindered internal wave. In the first 20 seconds, tests for Fr_{air} 0.80 and 0.95 show similar attenuation of the exchange flow. A higher air

flow rate ($Fr_{air} 1.1$) increases mixing. This shows that increasing the air flow rate does not necessarily improve the performance of the bubble screen as mitigating measure.

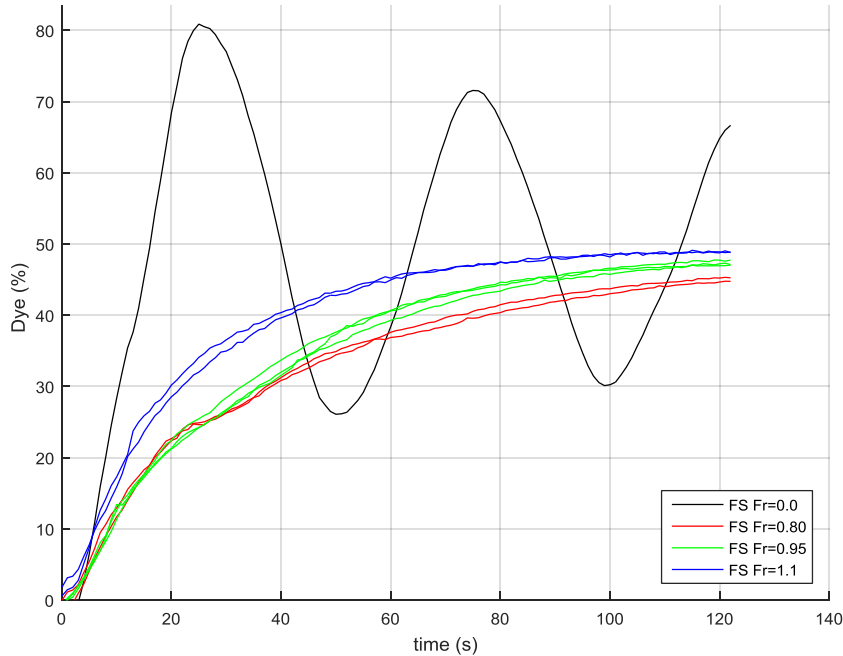


Figure 11: The salt mass in the left compartment of the tank, with varying air flow rate (Fr_{air} number), as a function of time (from Van der Ven and Oldenziel, 2018)

Van der Ven and Wieleman (2017) and Van der Ven and Oldenziel (2018) present scale experiments performed at a relatively small scale. To understand the scaling laws governing model tests on bubble screen performance, tests at larger scales may be necessary. Furthermore, future tests may comprise alternative bubble screen designs or further vary the applied air flow rate in order to show room for optimization.

4.3 Near-field numerical simulations

A third research method with great potential is the application of Computational Fluid Dynamics (CFD). An example is found in Meerkerk et al. (2015). In this research multiphase CFD models were applied to bubbly flows of different scales to judge their applicability. A successful validation was made for lab scale experiments of a bubble screen without density differences. The laboratory results were taken from literature, Wen and Torrest (1987). These experiments were made in a tank as illustrated in Figure 12, with dimensions $L = 3.7$ m, $W = 1.2$ m and $D = 0.9$ m. The bubble screen was made of a tube with holes, this was modelled in the CFD as a slit with $D_{in} = 0.02$ m. These dimensions are similar in order to the experiments performed at Deltares, described in the Paragraph 4.2.

The Computational Fluid Dynamics model uses a multiphase model in an Eulerian-Eulerian framework to describe the motion of both water and air (bubbles). In this framework the bubbles are not modelled explicitly but rather the domain is separated into control volumes (cells) in which the volume fraction of water and air in each cell is tracked. Momentum equations for both water and air are solved. These equations are coupled to each other with a multiphase interaction model. This includes the effects of buoyancy, entrainment, bubble lift and bubble drag. In this research the turbulence in the fluid is modelled using a Reynolds-Averaged Navier Stokes approach as this is the most applied and feasible for practical application. Other studies for bubble plumes have used an Eulerian-Lagrange framework (Fraga et al., 2016), where bubbles or parcels of bubbles are tracked

as particles moving through (and coupled with) the water. Similarly turbulence has been modelled with Large-Eddy Simulation (also Fraga et al., 2016). Both these approaches use far greater computational resources than those studied in Meerkerk et al. (2015) for bubble screens in locks.

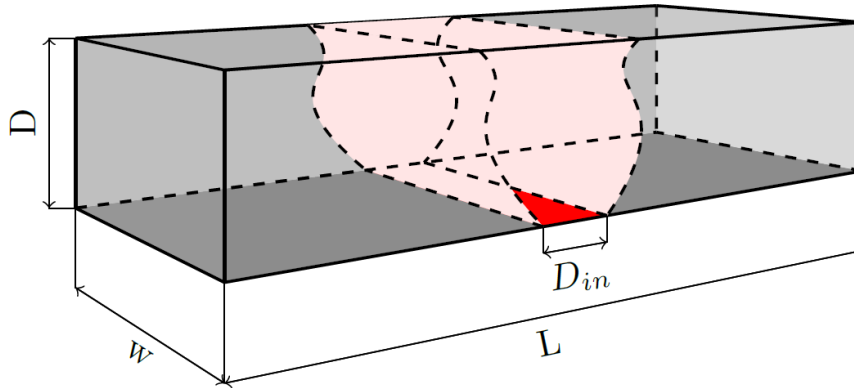


Figure 12: Illustration of the experimental tank used in Wen and Torrest (1987)

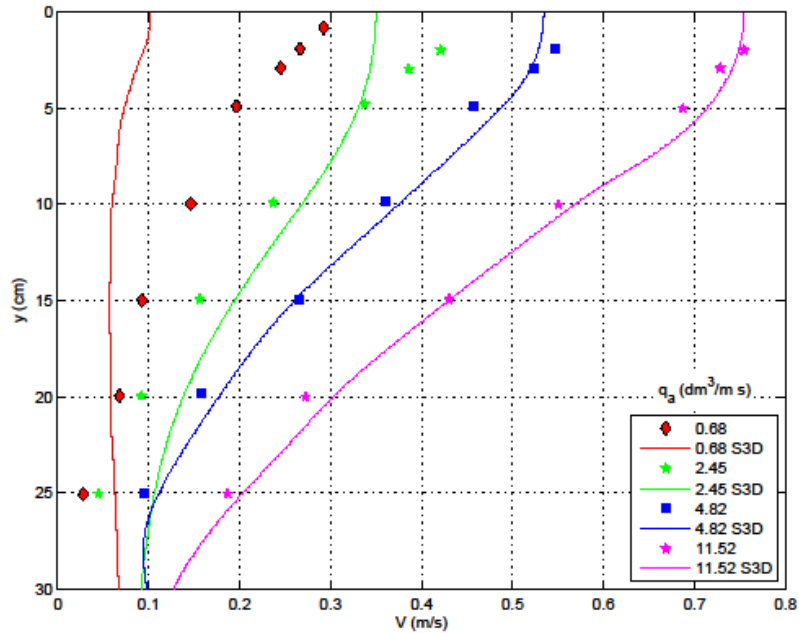


Figure 13: Results of the validation by Van Meerkerk et al. (2015)

The results of the validation in Meerkerk et al. (2015) are shown in Figure 13. For 4 different air flow rates the velocity profiles of the water in the top 30 cm of water (in a 90 cm water depth) are plotted at a distance 60 cm away from the axis of the bubble screen. These profiles are measured in the area away from the bubbles as the bubbles themselves often interfere with measuring equipment and the velocity profile at this offset location gives enough information about the water entrained in the bubble screen on its upward trajectory to assess the strength and effectiveness of the screen. CFD results can more easily give results at many locations in the domain but the validation has to be performed at the locations where measurements are available. The agreement in Figure 13 for the higher flow rates is good. For the lower flow rates the model performs badly.

Note that this model and validation is only for a bubble screen in freshwater and in steady state. The validation of a CFD model of a bubble screen as a barrier for salt intrusion has not as yet been

attempted but the experiments at Deltares described in Paragraph 4.2 are the first data set with sufficient data to provide a validation set for CFD. Thus far only qualitative CFD simulations have been made where a bubble screen has been combined with a density flow from saltwater-freshwater interactions (see Figure 14).

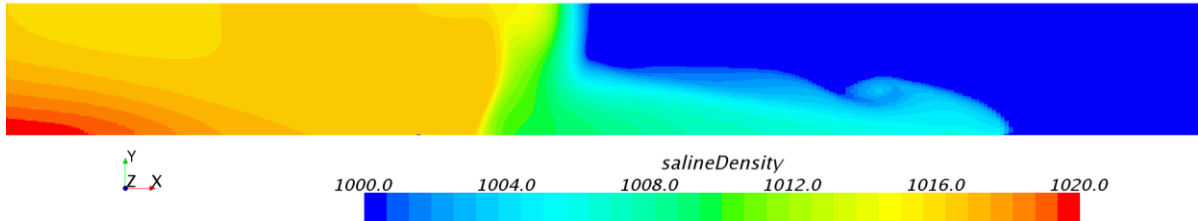


Figure 14: Result of a CFD computation of a bubble screen combined with a density flow

5. CONCLUSIONS

Salt intrusion through shipping locks is a concern at locations where restrictions on the salinity of inland waters apply due to ecological reasons or intake requirements for drinking water. This paper presents the main parameters affecting salt intrusion during the operation of sea locks, of which the number of lockages per day, the density difference over the lock and the dimensions of the lock are the most important. Based on this, it is easy to recognize the increasing relevance of research on salt intrusion given the global trends of increasing lock sizes and increasing traffic intensity.

Bubble screens are one of the possible measures to mitigate salt intrusion. This paper has focused on bubble screens but has also mentioned their performance when combined with a flushing discharge through the lock and/or water screens. Such combinations, and different bubble screen designs and operation have been tested in in-situ measurements that have been briefly presented here. These studies show that the salt transmission factor of bubble screens can reach as low as 0.25, which means that the lock exchange occurs four times as slow as it would in an unprotected lock. It is important to note that bubble screens reduce the speed of the process but cannot fully prevent lock exchange.

The performance of a bubble screen can be investigated a priori using scale model tests and/or numerical computations. This paper presents recent studies that evaluate and improve these methods, among which a scale model research that provides detailed data for the validation of numerical computations. These developments are currently ongoing.

When considering an intake point somewhere in a freshwater canal or lake, one should take into account not only the salt transmission factor η , but also the operation of the lock and the dispersion of the salt within the inland system. The effect of the bubble screen in terms of the reduction of salt intrusion resulting from successive lockages can be much greater than only a narrow consideration of the salt transmission ratio η . This paper presents a simplified method to compute the salt intrusion of successive lockages. The discussion given on the effect of door opening times is important as lock exchange will continue as long as the door is opened, albeit at a reduced rate when using bubble screens.

ACKNOWLEDGEMENTS

This paper presents studies commissioned by Rijkswaterstaat as well as research funded by the Dutch Ministry of Economic Affairs, through their TKI Deltatechnology program.

REFERENCES

- Abraham, G. and Van den Burg, P. (1962), Reduction of salt water intrusion through locks by pneumatic barriers, Delft Hydraulics Laboratory, Publication no. 28
- Abraham G, Van der Burgh P. and De Vos P. (1973), Pneumatic Barriers to Reduce Salt Intrusion through Locks, Rijkswaterstaat communications no. 17
- Boer, L. de , (2017), In welke mate kan optimalisatie van de schutoperatie bijdragen aan het beperken van zoutindringing door schutsluizen?, BEng thesis, Hogeschool Rotterdam (in Dutch)
- Boschetti, T., O'Mahoney, T.S.D., Bijlsma, A.C. (2017), CFD modelling of the mitigation of salt intrusion by selective withdrawal, 4th International Symposium on Shallow Flows (ISSF), 26-28 June 2017, Eindhoven, The Netherlands
- Van der Burg, P. and De Vos, P. (1962), Luchtbellenschermen in schutsluizen, Rijkswaterstaat (in Dutch)
- Bulson, P.S. (1961), Currents Produced by an Air Curtain in Deep Water – Report on Recent Experiments at Southampton, Dock and Harbour Authority, 1961, Vol. 42, Nr. 287, pp. 15-22
- Fraga, B., Stoesser, T., Lai, C.C.K. and Socolofsky, S.A. (2016), A LES-based Eulerian Lagrangian approach to predict the dynamics of bubble plumes, Ocean Modelling, 97, pp. 27-36
- Gans, O.B. de, (2010), SIVAK II Handleiding, Rijkswaterstaat (in Dutch)
- Groot, I. de (2015). WANDA-Locks, het nieuwe zoutlekmodel, Deltares report 1209463-000-HYE-0002 (in Dutch)
- Keetels G., Uittenbogaard R., Cornelisse J., Villars N., Pagee H. van (2011), Field study and supporting analysis of air curtains and other measures to reduce salinity transport through shipping locks, Irrigation and Drainage, 60 (Suppl. 1), 42–50
- Meerkerk, M. van, O'Mahoney, T., Twerda, A. (2015), Development of a CFD Model of an Air Curtain for Saltwater Intrusion Prevention, 36th IAHR World Congress, 28 June-3 July 2015, The Hague, The Netherlands
- Riess, I.R., and Fanneløp, T.K. (1998), Recirculating flow generated by line-source bubble plumes, Journal of Hydraulic Engineering, 1998.124:932-940
- Shin, J.O., Dalziel, S.B. and Linden, P.F. (2004), Gravity currents produced by lock exchange, Journal of Fluid Mechanics, vol. 521, pp. 1-34
- Uittenbogaard R.E. (2010), Voorstudie: ontwerpstudie en praktijkproef zoutlekbeperving Volkeraksluizen – Model voor zoutvracht-berekeningen. Deltares report 1201226-011-ZKS-0002 (in Dutch)
- Uittenbogaard, R., Cornelisse, J. and O'Hara, K. (2015a), Water – Air Bubble Screens Reducing Salt Intrusion through Shipping Locks, 36th IAHR World Congress, 28 June-3 July 2015, The Hague, The Netherlands
- Uittenbogaard, R., (2015b), Reduction of Salt Intrusion Through Shipping Locks, PAO Stroming en Golven rond Waterbouwkundige Werken, Lecture slides, 21 May 2015

Van der Ven, P.P.D., De Groot, I., Vreeken, D.J. and Weiler, O.M. (2015), Simulating Lock Operations in the Generic Salt Intrusion Model WANDA-Locks, 7th PIANC-SMART Rivers Conference, 7-11 September 2015, Buenos Aires, Argentina

Van der Ven, P.P.D. and Oldenziel, G. (2018), A Scale Model Study Assessing the Performance of a Bubble Screen Mitigating Salinity Driven Lock Exchange, 5th IAHR Europe Congress, 12-14 June 2018, Trento, Italy

Van der Ven, P.P.D. and Wieleman, V.A. (2017), The use of small scale experiments for a shipping lock's bubble screen, 4th International Symposium on Shallow Flows (ISSF), 26-28 June 2017, Eindhoven, The Netherlands

Vrijburcht, A. et al. (2000), Ontwerp van schutsluizen (Deel 2), Bouwdienst Rijkswaterstaat, ISBN 9036933056 (in Dutch)

WANDA, <https://www.deltares.nl/en/software/wanda/>

Weiler, O., Van de Kerk, A.J. and Meeuse, K.J. (2015), Preventing Salt Intrusion through Shipping Locks: Recent Innovations and Results from a Pilot Setup, 36th IAHR World Congress, 28 June-3 July 2015, The Hague, The Netherlands

Weiler, O.M., Zoutindringing door Kunstwerken – NKvdT 2017 – Schutsluizen, Deltares report 11200741-003 (in Dutch)

Wen, J. and Torrest, R.S. (1987). Aeration Induced Circulation From Line Sources. I: Channel Flows, J. Environ. Eng. Vol. 113, 82-98.